

Gating Kinetics of Ca²⁺-activated K⁺ Channels from Rat Muscle Incorporated into Planar Lipid Bilayers

Evidence for Two Voltage-dependent Ca²⁺ Binding Reactions

EDWARD MOCZYDLOWSKI and RAMON LATORRE

From the Department of Physiology and Biophysics, Harvard Medical School, Boston, Massachusetts 02115

ABSTRACT The gating kinetics of a Ca²⁺-activated K⁺ channel from adult rat muscle plasma membrane are studied in artificial planar bilayers. Analysis of single-channel fluctuations distinguishes two Ca²⁺- and voltage-dependent processes: (a) short-lived channel closure (<1 ms) events appearing in a bursting pattern; (b) opening and closing events ranging from one to several hundred milliseconds in duration. The latter process is studied independently of the first and is denoted as the primary gating mode. At constant voltage, the mean open time of the primary gating mode is a linear function of the [Ca²⁺], whereas the mean closed time is a linear function of the reciprocal [Ca²⁺]. In the limits of zero and infinite [Ca²⁺], the mean open and the mean closed times are, respectively, independent of voltage. These results are predicted by a kinetic scheme consisting of the following reaction steps: (a) binding of Ca²⁺ to a closed state; (b) channel opening; (c) binding of a second Ca²⁺ ion. In this scheme, the two Ca²⁺ binding reactions are voltage dependent, whereas the open-closed transition is voltage independent. The kinetic constant derived for this scheme gives an accurate theoretical fit to the observed equilibrium open-state probability. The results provide evidence for a novel regulatory mechanism for the activity of an ion channel: modulation by voltage of the binding of an agonist molecule, in this case, Ca²⁺ ion.

INTRODUCTION

The opening and closing process of ion channels is regulated by two distinct physiological mechanisms: transmembrane electrical potential or binding of

Address reprint requests to Dr. Edward Moczydlowski, Dept. of Biochemistry, Brandeis University, Waltham, MA 02154. Dr. Latorre's present address is Dept. of Biology, Faculty of Basic and Pharmaceutical Sciences, University of Chile, Santiago, Chile.

an agonist molecule. For example, the fluctuation rates of Na⁺ channel (Sigworth and Neher, 1980) and delayed rectifier (Conti and Neher, 1980) are modified by an applied voltage, whereas gating and desensitization kinetics of acetylcholine receptor channels are mediated by binding of acetylcholine (Sakmann et al., 1980). Recently, a high conductance (200–230 pS) K⁺-selective channel that is activated by both voltage and Ca²⁺ ions has been observed by patch-clamp recording from diverse biological preparations: bovine chromaffin cells (Marty, 1981), rat myotubes (Pallotta et al., 1981; Methfessel and Boheim, 1982), anterior pituitary cells (Wong et al., 1982), and vertebrate neurons (Adams et al., 1982). A similar channel has been studied in artificial planar bilayers by incorporating vesicles derived from transverse tubule of rabbit skeletal muscle into planar membranes (Latorre et al., 1982). For all cases studied in detail, both Ca²⁺ and voltage activate these channels by increasing the fraction of time the channel spends in the open state (Latorre et al., 1982; Barret et al., 1982; Wong et al., 1982; Methfessel and Boheim, 1982). The properties of high conductance and selectivity, combined with the ubiquitous presence of the channel in different cells and the possibility of *in vitro* assay systems, make this channel an attractive system in which to investigate the mechanism of voltage- and agonist-dependent gating.

In the present study, we analyze the gating behavior of a similar Ca²⁺-activated K⁺ channel incorporated into planar phospholipid bilayers from a vesicular preparation of plasma membrane from rat skeletal muscle. Pure phosphatidylethanolamine bilayers are used to minimize possible effects of surface charge on Ca²⁺ binding in membranes containing negatively charged lipid (McLaughlin, 1977). We find that the reconstituted channel in decane-containing bilayers behaves in a manner remarkably similar to that of the channel from rat myotubes previously described in native membrane patches (Barret et al., 1982; Methfessel and Boheim, 1982) and to that of the rabbit T-tubule channel characterized in artificial membranes (Latorre et al., 1982). We are able to derive a complete set of kinetic constants for a gating model in which the voltage dependence resides in the Ca²⁺ binding reactions. The first-order rate constants for the closed-open conformational transition are found to be voltage independent within the resolution of our methods. Several alternative molecular models that may account for voltage-dependent Ca²⁺ binding to activation sites on a transmembrane integral protein are discussed.

MATERIALS AND METHODS

Membrane Preparation and Planar Bilayer System

Plasma membrane vesicles from adult rat skeletal muscle were prepared by the method of Roseblatt et al. (1981). This preparation has been characterized as transverse tubule membrane with contaminating amounts of surface sarcolemma by measuring ouabain and saxitoxin binding activities (Moczydlowski and Latorre, 1983). Membrane suspensions (5–10 mg proteins/ml in 0.3 M sucrose) were stored

in small samples at -70°C and thawed as needed. Channel incorporation can be observed with thawed samples stored up to 1 wk on ice.

Planar bilayers were formed by the Mueller and Rudin (1969) technique using 20 mM phospholipid in decane. The lipid solution was painted on 200- μm holes in a polystyrene partition. Pure bovine brain phosphatidylethanolamine (PE) was used to form bilayers. Membrane capacitance was 100–200 pF.

Single-channel membranes were obtained by adding 5–20 μg protein to one side (*cis*) of a preformed bilayer separating 2.5-ml (*cis*) and 4.5-ml (*trans*) chambers containing 10 mM MOPS-Tris, pH 7.0, 0.1 M KCl, and 1 mM β -mercaptoethanol. To promote channel incorporation, an osmotic gradient was created by adding 0.1 M KCl to the *cis* chamber with constant stirring. After incorporation, 0.1 M KCl was added to the *trans* chamber, giving a final symmetrical KCl concentration of 0.2 M. The CaCl_2 concentration was varied from 1 μM to 10 mM by consecutive additions of stock solutions to the *cis* chamber. *trans* CaCl_2 tested up to 1 mM had no effect on the gating kinetics. CaCl_2 concentrations were determined by atomic absorption spectrophotometry. Experiments were performed at ambient temperature, 20–22 $^{\circ}\text{C}$.

The voltage-clamp circuit for measuring single-channel currents was as previously described (Latorre et al., 1982), using an LF157 operational amplifier (National Semiconductor, Santa Clara, CA) with a 10^8 - Ω feedback resistor. Voltage is referred to the *cis* chamber; the *trans* chamber is virtual ground. Practical time resolution of this system was limited to 4–5 kHz by current noise from the bilayer. For analysis of the primary gating mode, 1 kHz resolution was sufficient.

For kinetic experiments, single-channel fluctuations were recorded on magnetic tape with a 4D 4714 FM recorder (Lockheed, Sarasota, FL) at 30 in./s (10 kHz). For the experiments of Fig. 14, steady state current was recorded directly on a chart recorder by heavily filtering channel fluctuations with a 1-Hz RC passive circuit.

Data Analysis

Only single-channel membranes were used for detailed stochastic analysis. We confirmed that membranes contained only one channel by checking that there was a single open-state level at open-state probabilities approaching 1.0, i.e., high Ca^{2+} and positive voltages. Populations of dwell time events in either the open (290 ± 30 pS at 0.2 M KCl) or closed (zero conductance) states were analyzed using a MINC 11/23 computer (Digital Equipment Co., Marlboro, MA). Current records filtered at 1–4 kHz were digitized at sampling rates of 1,000–4,000 points/s. Open-state and closed-state events were identified by setting a discriminator at 50% of the open-state current. Cumulative probability distribution histograms were constructed by consecutive addition of points to a number vs. time array for each event. Probabilities were normalized to unity by dividing the total number of events, typically in the range of 200–1,000 for 20 s of channel time. Where indicated, short-lived closing events (“flickers”) were excluded from the analysis by counting a closing event lasting <1 ms as part of the preceding open-state event.

In addition to rapid fluctuations between closed- and open-state levels on a millisecond time scale, we have observed that Ca^{2+} -activated K^+ channels from rat muscle membrane preparations sometimes exhibit closing events of up to several seconds in duration. Fig. 1A shows an example of such a slow closure. This phenomenon has been previously described for a similar preparation from rabbit muscle (Latorre et al., 1982) and also by other laboratories using patch-clamp techniques (Barret et al., 1982; Methfessel and Boheim, 1982). These events were studied

independently of the primary gating activity and were well described by an analysis based on voltage-dependent blockade by Ca^{2+} . We refer to the accompanying paper for a detailed study of this phenomenon (Vergara and Latorre, 1983). Because slow closures are best treated as a separate phenomenon, closing events lasting longer than 500 ms were excluded from the present analysis. Fewer than 10 of such events were actually rejected from many thousands of transitions that were analyzed. Our laboratory and others (Barret et al., 1982; Methfessel and Boheim, 1982) have also noted a rare substrate conductance level of $\sim 50\%$ of the full open state, lasting as long as 50 ms in duration (e.g., Fig. 1*B*). The appearance of this state was less frequent than the slow closures and did not appear to vary with voltage or Ca^{2+} concentration. No attempt was made to exclude such events in the computer analysis of the open- and closed-state populations. Because of their rarity, neither the slow closure nor the substate phenomenon could significantly affect our results.

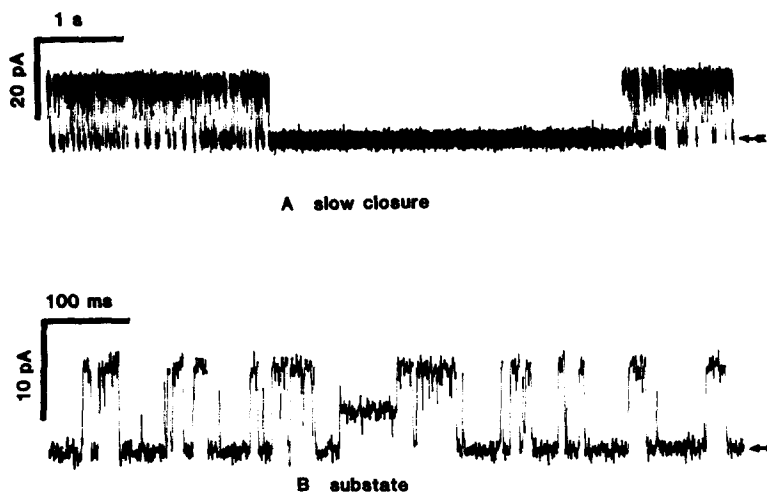


FIGURE 1. Examples of slow closure events and substate conductance levels. Conditions: (A) $5 \mu\text{M Ca}^{2+}$, $+50 \text{ mV}$; (B) $3 \mu\text{M Ca}^{2+}$, $+30 \text{ mV}$. 1 kHz filtering. Zero-current levels are indicated by the arrow to the right of each trace.

A more serious problem that could affect our analysis of channel gating was variation in the Ca^{2+} concentration dependence and voltage dependence from channel to channel. The extent of this variation is described in more detail in the Results section. In addition to sample variation, we sometimes observed sudden or graded shifts in the open-state probability that may or may not return to the previous level (e.g., see Fig. 15). Because of these observations, we cannot assume that lifetime data from a random sampling of different channels can be averaged. Therefore, in our analysis of the primary gating mode, we analyzed data individually from single-channel membranes that exhibited relatively stable gating behavior. These were studied over a wide voltage ($+60$ to -60 mV) and Ca^{2+} concentration ($1 \mu\text{M}$ to 10 mM) range. The microscopic kinetic results are based on an analysis of four different single channels (a total of 72 different Ca^{2+} concentration and voltage combinations). In addition, the voltage and Ca^{2+} concentration dependencies of 40 different bilayers, each containing one to four channels, were analyzed at a macroscopic level by recording steady state current (e.g., experiments of Fig. 14) to confirm that results

at the microscopic level were representative of the population of channels in the preparation.

Materials

PE was from Avanti Polar Lipids (Birmingham, AL), decane was from Eastman Organic Chemicals (Rochester, NY), and KCl was puratronic grade from Alfa Division, Ventron Corp. (Danvers, MA).

RESULTS

Identification and Analysis of the Primary Gating Mode

Figs. 2 and 3 are representative 800-ms segments of records from a single

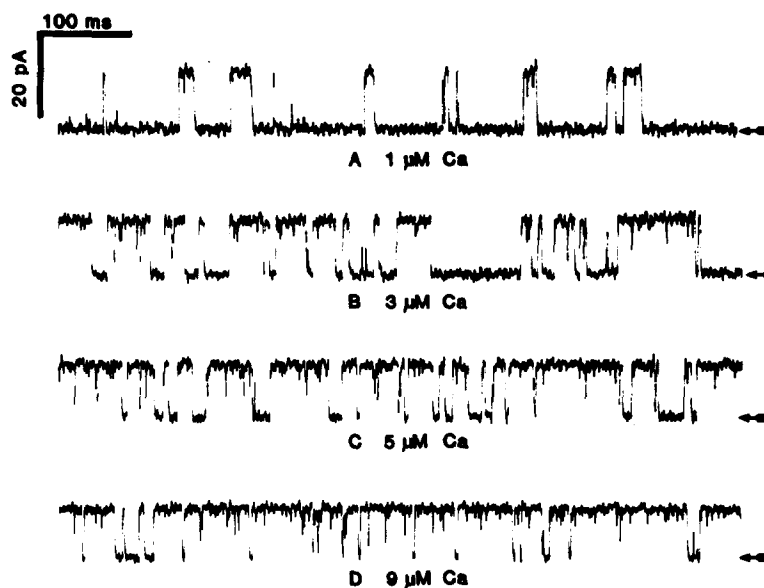


FIGURE 2. Effect of Ca²⁺ concentration on single-channel current fluctuations at constant voltage. Fluctuations from a pure PE bilayer were recorded at a holding voltage of +40 mV and the indicated concentration of *cis* CaCl₂. The measured probabilities of residence in the open state, averaged over 20 s, were: (A) 0.22; (B) 0.66, (C) 0.81; (D) 0.93. Zero-current levels are indicated by the arrow to the right of each trace. Time proceeds from left to right in all current records. 1 kHz filtering.

channel that illustrate the effect of Ca²⁺ concentration and membrane potential, respectively. Fig. 2 shows that as Ca²⁺ concentration is increased at fixed voltage, the time-averaged probability of residing in the open state, P_o , is increased from zero at low Ca²⁺ to values close to unity at high Ca²⁺ (Latorre et al., 1982). Fig. 3 shows that as the holding voltage is made more positive at a fixed Ca²⁺ concentration, P_o is also increased in a similar fashion. This behavior has been analyzed previously in terms of a two-state, closed-open, voltage-dependent equilibrium which predicts that P_o is a sigmoid function

of membrane potential that shifts along the voltage axis as a function of Ca^{2+} concentration (Latorre et al., 1982; Methfessel and Boheim, 1982; Wong et al., 1982). The present goal is to develop a kinetic model able to predict both the microscopic and macroscopic behavior of the channel.

We analyzed the Ca^{2+} activation of this channel following the approach described for agonist-activated channels by Colquhoun and Hawkes (1981). The strategy involves measuring the mean open and closed times as a function of agonist concentration, i.e., Ca^{2+} concentration. Since different kinetic schemes predict unique relationships for the mean open and closed times vs. agonist concentration, the most economical scheme that predicts the observed relationships might be identified.

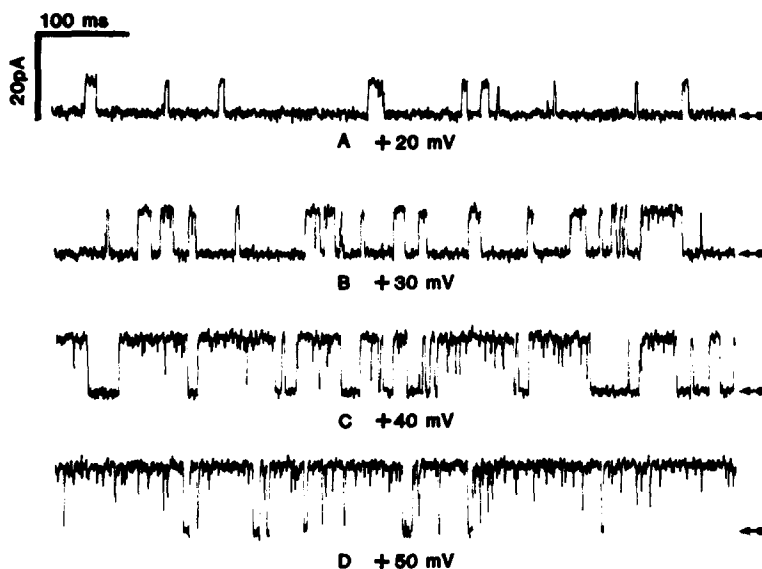


FIGURE 3. Effect of applied membrane potential on single-channel fluctuations at constant Ca^{2+} concentration. Fluctuations from the same channel as that of Fig. 1 are shown at $3 \mu\text{M}$ *cis* CaCl_2 and the indicated holding voltages. The time-averaged open-state probabilities were: (A) 0.16; (B) 0.29; (C) 0.66; (D) 0.87. 1 kHz filtering.

Fig. 4 illustrates the method used to identify the primary gating mode and to measure the mean open and closed dwell times for these states. Fig. 4A shows a segment of a record from the same channel of Figs. 2 and 3 at a 4-kHz resolution and expanded time scale. Simple inspection of this record reveals that there are two types of closing events. One type consists of well-resolved closed-state events, while the second type consists of short-lived clustered spikes or "flickers" emanating from the open-state level in a bursting pattern. Most of these flicker events are not fully resolved even at 4 kHz, the practical limit of our recording system. Fig. 4B (lower curve) shows the cumulative probability distribution of residence times in the closed state resulting from computer compilation of 5 s of channel activity (422 events)

sampled at 4 kHz as described in Materials and Methods. This distribution clearly exhibits two components, as expected from simple inspection of the records. The long component, consisting of well-resolved closures, comprises

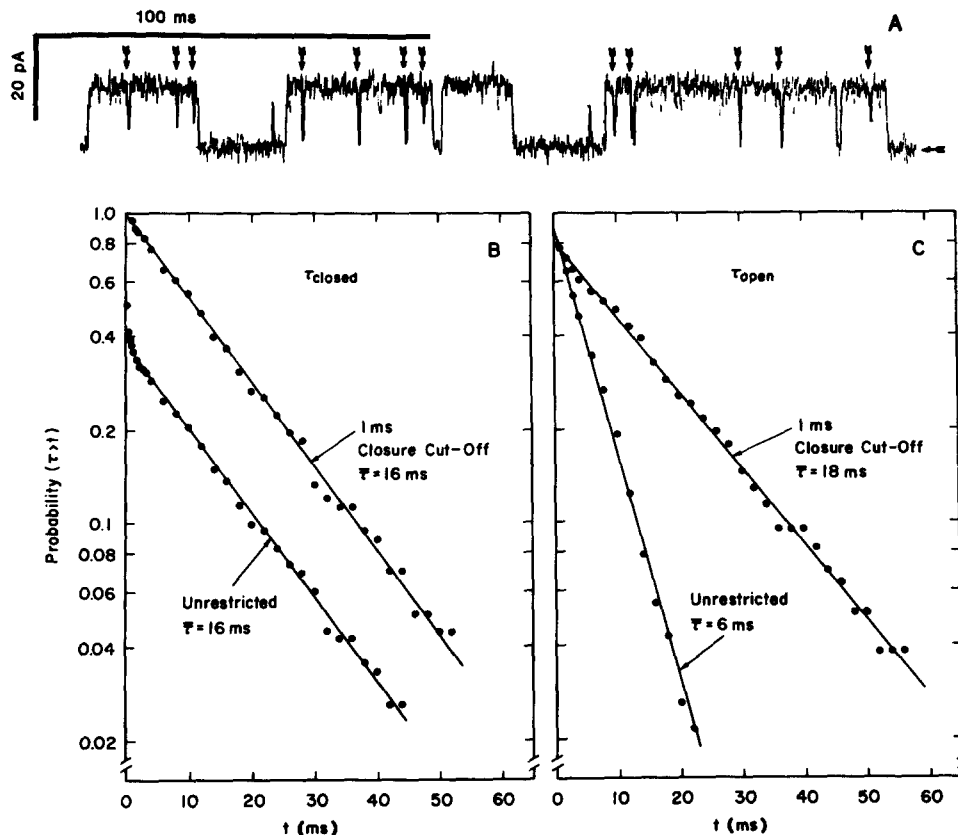


FIGURE 4. Effect of excluding flicker closures on the probability distributions of closed- and open-state dwell times. In A, part of a single-channel current record taken at +50 mV holding voltage and 1 μM *cis* Ca²⁺ is shown at 4 kHz filtering. Short-lived closing events ("flickers") that visually close to at least half of the open-state level are marked with a vertical arrow. The closed- (B) and open- (C) state cumulative probability distribution histograms of dwell times were tabulated by a computer program as described in Materials and Methods, after digitization of 5 s of analog input (4 kHz filtering) at 4,000 points from the same record shown in A. The lower distributions in B and C, labeled "unrestricted," count all transitions reaching 50% of the open-state level as events. The total number of events for these distributions was 422. The upper distributions in B and C were tabulated from the same data as that of the lower distributions, except that all closing events ≤ 1 ms in duration ("flickers") were counted as part of the preceding open-state event. The total number of events for these distributions was 158 after excluding 264 flicker events. Data points for each distribution are plotted at arbitrarily chosen intervals. For the purpose of illustration, straight lines were drawn by eye and the mean dwell times, $\bar{\tau}$, corresponding to these lines are given in the figure. See text for explanation.

37% of the population and has a mean of 16 ms. The 63% remaining events belong to the flicker population with a mean time of <0.4 ms. Because the flicker lifetime is very short, the channel spends only a small fraction of the total time in flicker events. However, it is possible that these events are in some way related to the kinetic pathway for channel activation and should ultimately be included as part of any complete kinetic scheme. As a method of facilitating the present analysis, the effect of ignoring the flicker events by treating them as part of the open state is investigated below.

In order to exclude the flickers, we empirically determined a minimum cut-off time for closing events that resulted in a single-exponential distribution of closed-state dwell times. Fig. 4*B* (upper curve) shows that by excluding all closing events <1 ms in duration, the fast component of the distribution is effectively eliminated, resulting in a distribution well fit by a single exponential with a time constant equivalent to the slower component of the unrestricted population (lower curve). Fig. 4*C* illustrates the effect of this procedure on the open-state distribution. The mean open time is increased (from 6 to 18 ms) after flickers are excluded since an opening event is terminated only after a closure >1 ms is counted. The open-state distribution is well fit by a single exponential at times >1 ms before and after flickers are excluded. However, there also appears to be an excess of short-lived opening events. This is indicated by an ordinate extrapolation of the data in Fig. 4*C* to 0.8 instead of 1.0. The two brief opening flickers in the record of Fig. 4*A* are likely examples of this 20% population of a fast component in the open state.

In Fig. 5, *A* and *B*, cumulative probability distributions for closed and open states constructed by excluding 1-ms closures are shown at several Ca^{2+} concentrations at fixed voltage (+20 mV). These results are typical for the complete range of Ca^{2+} concentrations (1 M to 10 mM) and holding potentials (+60 to -60 mV) we have investigated at 0.2 M KCl. We find that the populations of closed and open dwell times are well described by single-exponential distributions to the level of 2–5% of the events. We also find that the fast component of the open-state population is only detectable at the lower Ca^{2+} concentration range for any given voltage. This is indicated in Fig. 5*B* by ordinate extrapolations <1.0 at 1 and 3 μM Ca^{2+} . At most, these events comprise 20% of the population and do not strongly affect the overall mean. An interpretation for this behavior in the low Ca^{2+} limit will be provided in a later section of the Results.

In summary, we find that by excluding closures of <1 ms in duration, single-exponential distributions of the closed and open dwell times are unmasked (i.e., Fig. 5, *A* and *B*). We refer to this residual gating pattern as the primary gating mode, since the channel spends $>97\%$ of total time in this mode. In analyzing the primary gating mode by this method, the mean open time that we obtain is actually the mean burst length of openings separated by flicker closings. We also find that a sampling rate of 1 kHz for recorders filtered at 1 kHz is sufficient to resolve this primary gating mode,

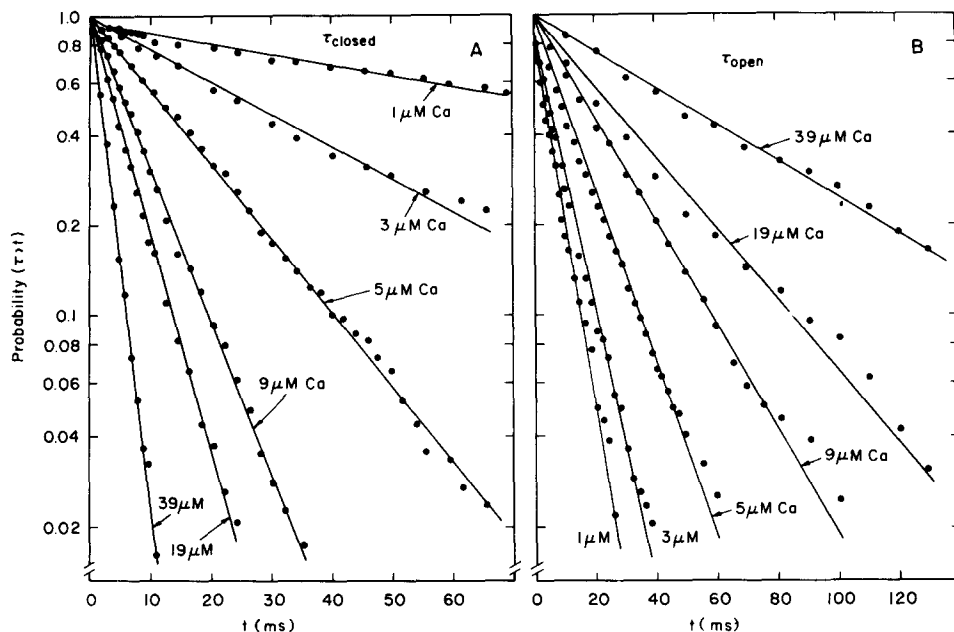


FIGURE 5. Closed- and open-state probability distributions for a single channel at various Ca^{2+} concentrations. Single-channel current fluctuations were recorded at +20 mV holding voltage and the indicated Ca^{2+} concentrations. Closed- (A) and open- (B) state cumulative probability distribution histograms obtained after digitization of 20 s of analog input (1 kHz filtering; sampling rate: 1,000 points/s). All closed events of 1 ms in duration (1-point "flickers") were counted as part of the preceding open-state event. Data points for each distribution are plotted at arbitrarily chosen intervals. Straight lines are drawn according to least-squares semilogarithmic fits of the data (correlation coefficients were 0.99). The corresponding mean closed and mean open times for these distributions (determined both as the simple average and the mean given by the least-squares fit) are plotted in Figs. 6A and 7A, labeled as "+20 mV." The measured time-averaged probability of open-state residence, P_o , was: 1 μM , 0.06; 3 μM , 0.16; 5 μM , 0.44; 9 μM , 0.73; 19 μM , 0.82; 39 μM , 0.95. The total number of events measured for each distribution was: 1 μM , 183; 3 μM , 386; 5 μM , 591; 9 μM , 571; 19 μM , 456; 39 μM , 246.

since probability distributions accumulated under these conditions are equivalent to those taken at 4 kHz, when flickers are excluded.¹

¹ By sampling at 1 kHz and excluding 1-ms closures from the closed-state population, we are effectively limited to conditions in which the overall mean closed time is >3 ms. As the extreme of short closed times is approached (i.e., Fig. 2D), we risk overestimating the mean open time by excluding closures that do not belong to the population of flickers. Indeed, this method is only legitimate when the duration of flicker closures is well separated from the duration of inter-burst closures. Therefore, the analysis is restricted to conditions in which the mean open or mean closed time is >3 ms.

Identification of a Scheme Compatible with the Ca^{2+} Concentration Dependence of the Mean Dwell Times

Figs. 6A and 7A show the Ca^{2+} concentration dependence of the mean open and mean closed times, respectively, for a single channel studied at positive voltages, +20 to +50 mV. Figs. 6B and 7B show the same measurements for a different single channel studied at negative voltages, -20 to -60 mV. Since the probability distribution histograms are well fit by single-exponential functions, the average dwell time of the population should equal the time constant of a linear least-squares fit of the semilogarithmic histogram plots,

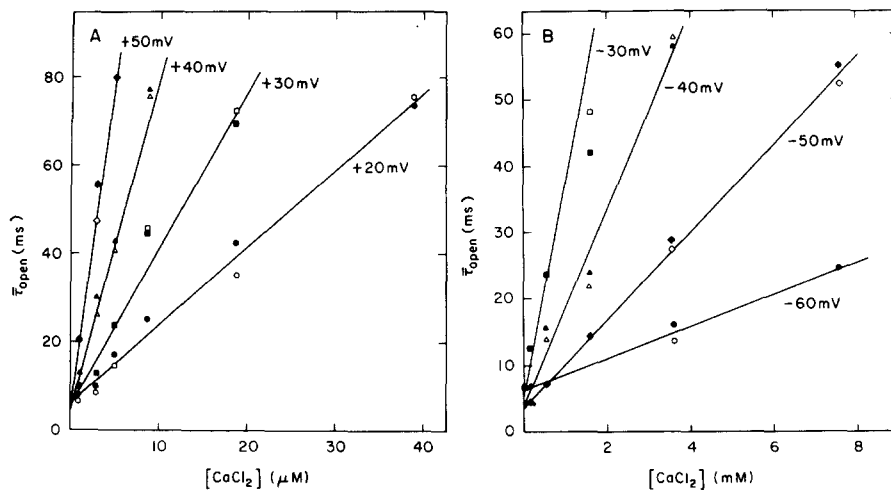


FIGURE 6. Linear relationship between the mean open-state dwell time and Ca^{2+} concentration at constant voltage. Single-channel current fluctuations were recorded at the indicated Ca^{2+} concentrations and holding voltages. The data were analyzed as described in Fig. 5. The mean open times calculated as a simple average (open symbols) or as the time constant of a least-squares semilogarithmic fit (closed symbols) are plotted vs. Ca^{2+} concentration. In cases where the two methods of obtaining the mean were equivalent, only a filled symbol is shown. Data shown in A (positive voltages) and B (negative voltages) were obtained from two different channels. Note the different abscissa scales for A vs. B.

as expected for a Poisson process. As a test of goodness of fit to a single exponential, the mean open and closed times are determined by both methods. The simple averages of the event populations are plotted as open symbols and the means determined by least-squares fitting are plotted as filled symbols in Figs. 6 and 7. In cases where the two values are identical, only a filled symbol is shown. The results of this comparison indicate that, in most cases, there is excellent agreement between the two methods of evaluating the mean dwell time. In the worst case, the two methods differ by 10%.

In Fig. 6 the mean open times ($\bar{\tau}_o$) are plotted vs. Ca^{2+} concentration, and in Fig. 7 the mean closed times ($\bar{\tau}_c$) are plotted vs. reciprocal Ca^{2+} concentra-

tion. The results show that at any given fixed voltage, $\bar{\tau}_o$ is a linear function of $[\text{Ca}^{2+}]$ and $\bar{\tau}_c$ is a linear function of $1/[\text{Ca}^{2+}]$. Similar data from a total of four different single-channel membranes confirmed the results shown in Figs. 6 and 7. The linear relationships of $\bar{\tau}_o \propto [\text{Ca}^{2+}]$ and $\bar{\tau}_c \propto 1/[\text{Ca}^{2+}]$ are found to hold over the range of open-state probabilities of 0.05–0.95, the range accessible to the present analysis because of the 1-ms resolution limit. Figs. 6 and 7 also show that the mean dwell times are strongly dependent on voltage. Surprisingly, however, at low Ca^{2+} concentrations the mean open times at different voltages tend to converge to the same value, and at high Ca^{2+} the mean closed times at different voltages tend to converge to the same value. This result has profound implications for the voltage dependence of the channel, as discussed in the next section.

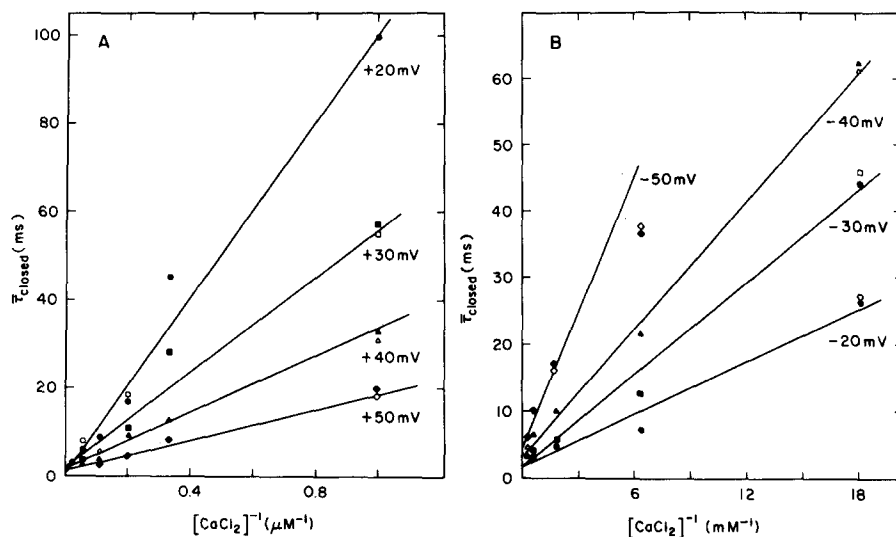


FIGURE 7. Linear relationship between the mean closed-state dwell time and reciprocal Ca^{2+} concentration at constant voltage. The data were collected and analyzed as described in Fig. 6.

We identify now a kinetic scheme of Ca^{2+} activation compatible with the data of Figs. 6 and 7. We investigated the predicted behavior of the different models without making any assumptions about the magnitude of the binding and rate constants and their voltage dependencies and without invoking the existence of charged gates or blocking particles (e.g., Methfessel and Boheim, 1982). One important fact that must be taken into account is the observation that the slope of Hill plots of the open-closed equilibrium vs. Ca^{2+} concentration is >1.0 , ranging from 1.2 at negative voltages to 1.8 at positive voltages (Fig. 11C). This result suggests that a minimum of two Ca^{2+} ions are bound to the channel for complete activation. Therefore, we will consider the general model of Fig. 8 for channel activation that includes the sequential binding of two Ca^{2+} ions to closed and open states with zero, one, or two

bound Ca^{2+} ions in reversible equilibrium. We assume that all closed states exhibit zero conductance, whereas all open states exhibit the same conductance value. From a thermodynamic standpoint, we cannot exclude any of the states shown in Fig. 8 for a channel that has two Ca^{2+} binding sites. However, it is possible that the probabilities for some of the states are small under normal conditions, so that we can effectively ignore them. Therefore, all possible subset pathways of the general model of Fig. 8 that include a state with two bound Ca^{2+} ions are examined to find the simplest scheme that accounts for our data. Several of these subset pathways, along with expressions for unconditional mean open and closed times as a function of Ca^{2+}

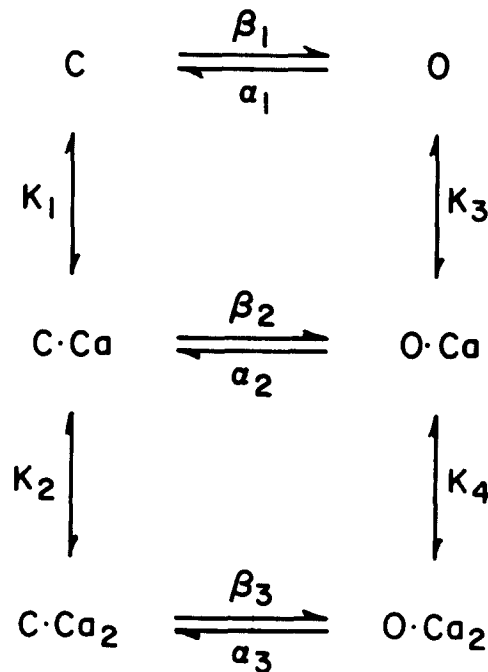




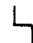
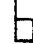

FIGURE 8. A general kinetic scheme for a channel that binds two Ca^{2+} ions. First-order conformational transitions between closed, C, and open, O, states are denoted by forward and reverse rate constants, β and α . Ca^{2+} binding reactions are denoted by dissociation equilibrium constants: K_1 , K_2 , K_3 , and K_4 .

concentration, are given in Table I. Expressions for $\bar{\tau}_o$ and $\bar{\tau}_c$ are obtained by methods outlined in Colquhoun and Hawkes (1977). Note that the schematic representation of model 5 of Table I corresponds to the general model of Fig. 8.²

² Although the mean dwell times given in Table I are general for any values of the rate constants, the form of the probability distributions with more than one closed or open state are sums of exponentials with amplitudes and time constants given by complex combinations of rate constants. The fact that we observe mean dwell times approximately equal to lifetimes of single-exponential decays suggests that if there are multiple open and closed states, a single-exponential term dominates the distribution. See the Appendix for a possible example of this behavior.

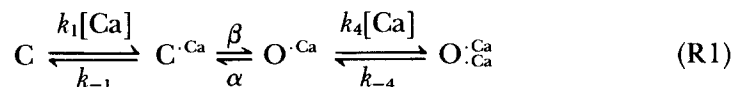
Inspection of the predicted Ca²⁺ concentration dependence of the various models in Table I reveals that model 3 contains the least number of kinetic states required to account for the data of Figs. 6 and 7. Models 1 and 2 are inadequate because in model 1 the mean open time is independent of [Ca²⁺] and in model 2 the mean closed time is independent of [Ca²⁺]. Model 3, however, predicts both that the mean open time is a linear function of Ca²⁺ concentration and that the mean closed time is a linear function of reciprocal Ca²⁺ concentration, in agreement with our observations. Models 4 and 5 are not the simplest models that explain our data because they predict that the mean open time approaches a limiting value at high Ca²⁺ concentration. On the other hand, model 5 predicts that the mean closed time has a limiting value at low Ca²⁺ concentration. Figs. 6 and 7 show no indication of such saturation behavior in these extremes; however, we cannot exclude the possibility that saturation might be observed at open-state probabilities be-

TABLE I
Dependence of the Mean Open or Closed Time on Ca²⁺ Concentration for Various Kinetic Models

Model	$\bar{\tau}_{\text{open}}$	$\bar{\tau}_{\text{closed}}$
1. 	α_3^{-1}	$\beta_3^{-1}(1 + K_2/C + K_1K_2/C^2)$
2. 	$\alpha_1^{-1}(1 + C/K_3 + C^2/K_3K_4)$	β_1^{-1}
3. 	$\alpha_2^{-1}(1 + C/K_4)$	$\beta_2^{-1}(1 + K_1/C)$
4. 	$\frac{1 + C/K_4}{\alpha_2 + \alpha_3C/K_4}$	$\frac{1 + C/K_1 + C^2/K_1K_2}{\beta_2C/K_1 + \beta_3C^2/K_1K_2}$
5. 	$\frac{1 + C/K_3 + C^2/K_3K_4}{\alpha_1 + \alpha_2C/K_3 + \alpha_3C^2/K_3K_4}$	$\frac{1 + C/K_1 + C^2/K_1K_2}{\beta_1 + \beta_2C/K_1 + \beta_3C^2/K_1K_2}$

The models shown are subset pathways of the general model of Fig. 8. Note that the schematic representation of model 5 corresponds to Fig. 8. Equations for the unconditional mean time in all open or closed states as a function of Ca²⁺ concentration and kinetic constants were derived by means of Eq. 74 in Colquhoun and Hawkes (1977). Note that C = [Ca²⁺]; K's are dissociation equilibrium constants. Not all the parameters are independent: $K_1\beta_1/\alpha_1 = K_3\beta_2/\alpha_2$; $K_4\beta_3/\alpha_3 = K_2\beta_2/\alpha_2$.

yond our resolution limit. Model 3 is advantageous because it is a simple linear kinetic scheme for which exact analytical expressions for the time dependent probability distribution functions of the various states can be obtained. From this point, we will consider the following scheme (model 3) in detail as a working hypothesis for the gating activation pathway:



Voltage Dependence of the Gating Reactions

Scheme R1 predicts the following linear relationships for the mean open and closed dwell times:

$$\bar{\tau}_o = \alpha^{-1}(1 + [\text{Ca}]/K_4); \bar{\tau}_c = \beta^{-1}(1 + K_1/[\text{Ca}]). \quad (1)$$

Eq. 1 allows us to derive the kinetic constants of scheme R1 by analyzing the slopes and intercepts of the straight lines shown in Figs. 6 and 7. According to Eq. 1, a plot of $\bar{\tau}_o$ vs. $[\text{Ca}^{2+}]$ has an ordinate intercept of $1/\alpha$ and a slope of $1/\alpha K_4$; a plot of $\bar{\tau}_c$ vs. $1/[\text{Ca}^{2+}]$ has an ordinate intercept of $1/\beta$ and a slope of K_1/β . Since the intercepts of the plots shown in Figs. 6 and 7 do not exhibit significant voltage dependence, whereas the slopes are strongly voltage dependent, we can conclude that most of the voltage dependence resides in the Ca^{2+} dissociation constants for the closed and open states. The ordinate intercepts, β^{-1} and α^{-1} , were obtained by linear regression from the mean closed and mean open time data, respectively, at various holding potentials. These results, obtained from four different channels, are shown in Fig. 9. The data of Fig. 9, A and B, indicate that β and α values for different channels and holding voltages tend to cluster about common mean values of $\beta = 480 \text{ s}^{-1}$ and $\alpha = 280 \text{ s}^{-1}$. These values for β and α and the mean dwell time data were used to obtain the Ca^{2+} dissociation constants for scheme R1, K_1 and K_4 , from Eq. 1.

The results of this analysis are shown in Fig. 10 for two different channels, where the most extensive data were collected. The K_1 and K_4 values for different Ca^{2+} concentrations are plotted individually to show the range of variation in the K values at a given holding potential. The K_1 and K_4 values from +60 to -60 mV are fit well by a simple-exponential function of voltage. Voltage-dependent binding constants can be explained by using the analysis of Woodhull (1973) for the case of ionic channel blockers. Using this analogy, we can express the voltage dependence of the K_1 and K_4 dissociation constants as:

$$K(V) = K(0) \exp(-z\delta FV/RT), \quad (2)$$

where $K(0)$ is the zero-voltage dissociation constant, z is the Ca^{2+} ion valence (+2), δ is the fractional distance of the electric field that is felt by the ion, and F , V , R , and T have their usual meanings. The data of Fig. 10 are fitted to Eq. 2 by an unweighted least-squares analysis to obtain values for $K(0)$ and δ , which are given in Table II.

The results of Fig. 10 and Table II indicate that the Ca^{2+} binding reaction to the closed state exhibits a lower affinity than the Ca^{2+} binding reaction to the open state, since K_1 is larger than K_4 at all measured voltages. However, as Fig. 10 shows, the difference in affinities is enhanced as the voltage is made more positive. According to our treatment, this is due to different δ values for the two binding reactions. The low-affinity binding site (K_1) is located at 70–80% ($\delta_1 = 0.67, 0.84$) of the electric field, whereas the high-affinity binding site (K_4) is located at 90–100% ($\delta_4 = 0.91, 1.0$) of the field.

Does Scheme R1 Predict Equilibrium Behavior?

From the preceding analysis of the dwell-time distributions of the open and closed states, we arrived at a model (R1) for the Ca^{2+} activation kinetics. The analysis also gave estimates of the rate constants (α , β) for the closed-open conformational transitions and explicit expressions (Eq. 3; Table II) for the

voltage-dependent Ca²⁺ binding dissociation constants (K_1 , K_4). It is of interest to evaluate the success with which scheme R1 can account for the equilibrium Ca²⁺ and voltage dependence of the probability of residence in the open state, P_o ($[Ca^{2+}]$, V). An explicit expression for this dependence can readily be derived from an equilibrium treatment of scheme R1, where P_o is equal

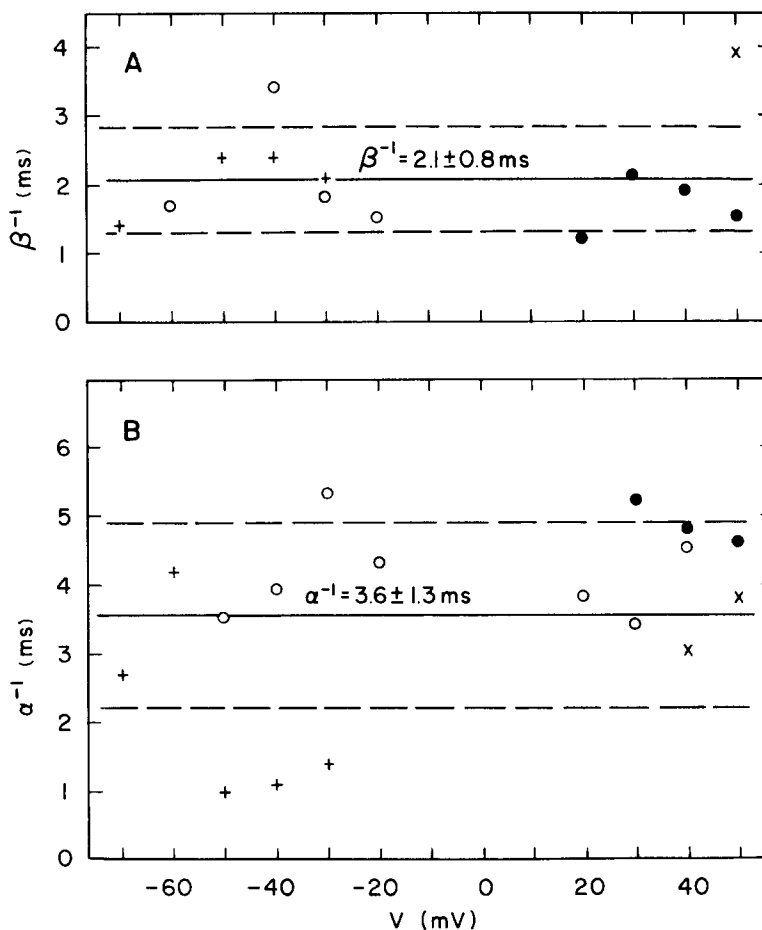


FIGURE 9. Voltage independence of first-order conformational transitions. The closing, α , and opening, β , rate constants of scheme R1 are given by the ordinate intercepts of plots shown in Figs. 6 and 7, respectively, according to Eq. 1. Ordinate intercepts were calculated as least-squares intercepts from mean open and closed time data at several Ca²⁺ concentrations from four different channels (O, ●, X, +) at the indicated holding voltages. The solid line indicates the mean values for the reciprocal opening rate constant, α^{-1} in A, and the reciprocal closing rate constant, β^{-1} in B, calculated as the simple average over all voltages. The limits of one standard deviation from the mean are shown as dotted lines. A few values greater than two standard deviations from the mean were discarded.

to the equilibrium ratio of the sum of the two open states over the sum of all the states. The resulting expression is:

$$P_o ([Ca^{2+}], V) = \frac{[Ca]^2 + [Ca]K_4}{[Ca]^2 + [Ca]K_4(1 + \alpha/\beta) + K_1K_4(\alpha/\beta)}, \quad (3)$$

where K_1 and K_4 are functions of voltage according to Eq. 2. It is worthwhile to note that Eq. 3 can also be derived from the expressions for the uncondi-

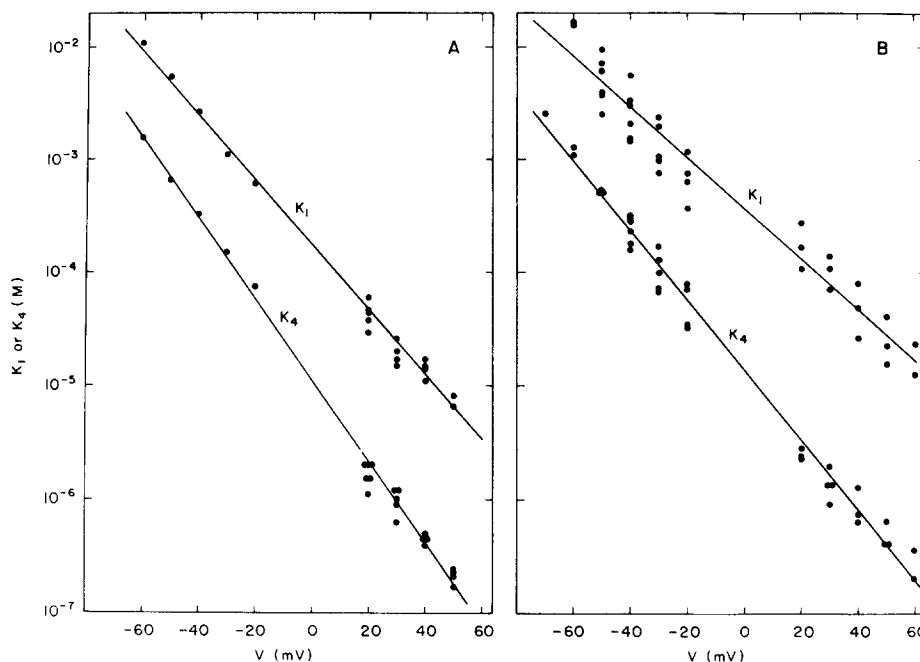


FIGURE 10. Voltage dependence of the two Ca^{2+} binding reactions of scheme R1. Ca^{2+} dissociation constants K_1 and K_4 of scheme R1 were calculated from mean closed and mean open time data, respectively, at various Ca^{2+} concentrations and holding voltages, using Eq. 1 given in the text. Mean open and mean closed times were obtained as described in Fig. 5. First-order rate constants, β and α , needed for these calculations were mean values determined in the experiment of Fig. 9. The solid lines are unweighted least-square fits. Parameters for these fits are given in Table II. Results in A and B were obtained from two different channels.

tional mean open and closed times for reaction scheme R1 by means of the relation

$$P_o ([Ca^{2+}], V) = \bar{\tau}_o / (\bar{\tau}_o + \bar{\tau}_c). \quad (4)$$

This equivalence is a simple illustration of the rationale for stochastic analysis: the microscopic behavior of a system is predicted by equilibrium thermodynamics.

Fig. 11 shows the results of a comparison of the theoretical Ca²⁺ concentration and voltage dependence of scheme R1 (using Eq. 3 and the best-fit values of α , β , K_1 , and K_4) with the actual experimental P_o values, measured as the fraction of time in the open state. The results for two different channels (Fig. 10, *A* and *B*) indicate close agreement between the calculated and measured open-state probabilities over the full range of [Ca²⁺] (1 μ M to 10 mM) and voltage (-60 to +60 mV) that was investigated. In particular cases, the theoretical curves either underestimated or overestimated the actual data by $\sim 0.1 P_o$ units. Discrepancies between the calculated and observed data appear to be random throughout the Ca²⁺ concentration range. Such deviations can be well explained by inherent instability of the gating behavior, described in a later section.

Kinetic Behavior in the Limit of Low Ca²⁺ Concentration

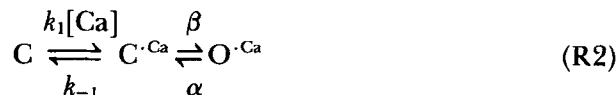
In the limit of low Ca²⁺ concentration, scheme R1 predicts that the probability of the doubly bound open state is low and that the mean open time approaches α^{-1} , the time constant for closing from the open state with one bound Ca²⁺.

TABLE II
Parameters for Two Voltage-dependent Ca²⁺ Binding Constants of Scheme R1

Channel	$K_1(0)$	δ_1	$K_4(0)$	δ_4
A	1.8×10^{-4} M	0.84	1.1×10^{-5} M	1.0
B	3.7×10^{-4} M	0.67	1.4×10^{-5} M	0.91

Zero-voltage dissociation constants, $K_1(0)$ and $K_4(0)$, and fractional distances of the electric field, δ_1 and δ_4 , for the two Ca²⁺ binding reactions of scheme R1 were determined by least-squares fitting of the data in Fig. 10 according to Eq. 1. Results for two different channels. A and B channels correspond to *A* and *B* of Figs. 10 and 11.

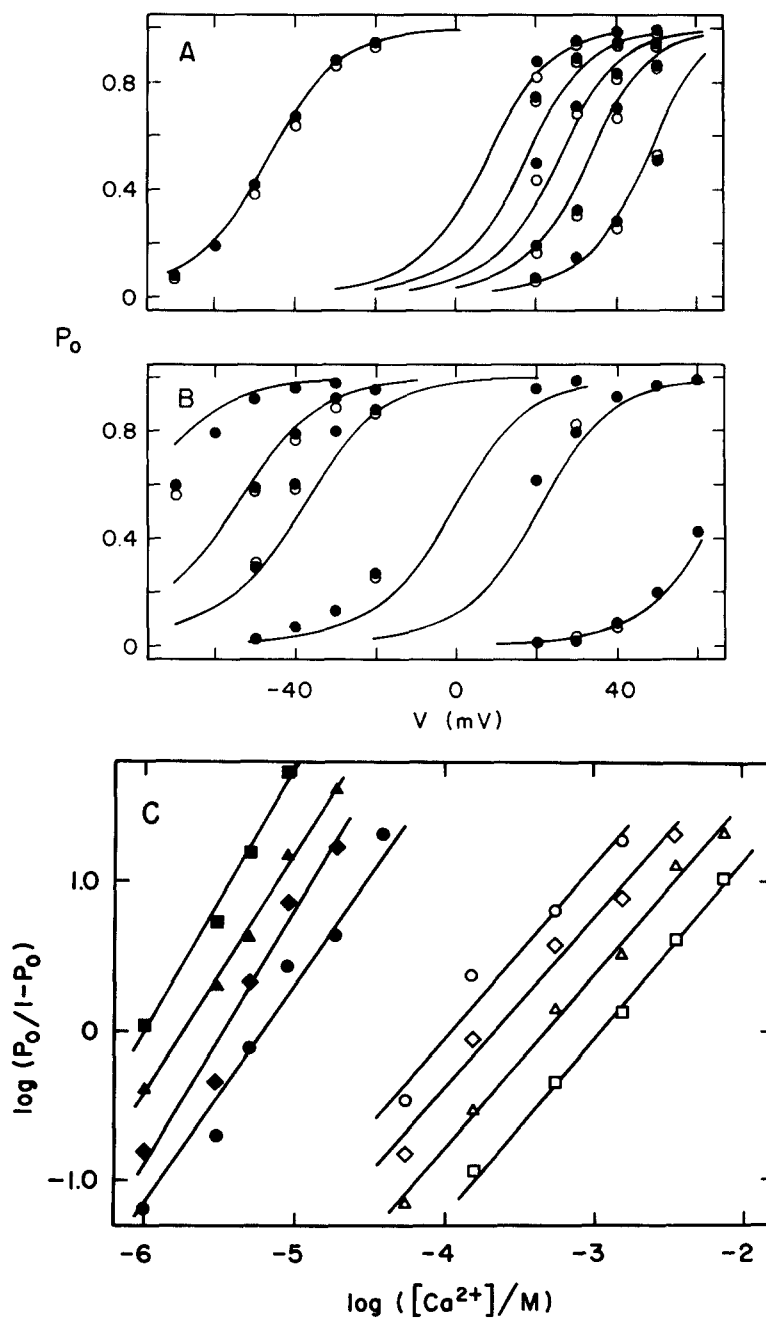
Also, the mean closed time increases in this limit, which reflects the fact that the rate constant for Ca²⁺ binding to the closed state, $k_1[\text{Ca}]$, becomes small enough to trap the channel in the unbound closed state, C, for long periods of time, as in the reduced reaction scheme:



Kinetic mechanisms such as scheme R2 are known to predict a bursting pattern of channel opening. Explicitly, the mean number of openings per burst is $(1 + \beta/k_{-1})$ and the mean length of closing events within a burst is $(\beta + k_{-1})^{-1}$ (Colquhoun and Hawkes, 1981). Thus, if β is large compared with k_{-1} , opening events tend to occur in closely spaced clusters.

We investigated the characteristics of the channel fluctuations at low Ca²⁺ concentration in an attempt to measure k_{-1} (see scheme R2). Fig. 12A shows a single-channel record taken at 1 μ M Ca²⁺, for which the time-averaged probability of the open state is $P_o = 0.024$. Under these

conditions, channel fluctuations appear as brief spikes with a mean open time of 2 ms. At a greater time resolution, two types of opening events can be resolved. The great majority of events are similar to those shown in Fig. 12B, simple open-closed transitions with no fine structure other



than background noise. In rare instances, some of the opening events are punctuated by brief closings, as shown in the examples of Fig. 12C. This latter type of events is possible evidence for bursting behavior in the low [Ca²⁺] limit.

Fig. 12D shows open- and closed-state probability distributions obtained for the record of Fig. 12A. The closed-state distribution exhibits a slow component comprising 90% of the population with a mean of 80 ms. Fig. 12D also shows a fast component that comprises the remaining 10% of the population. This latter component corresponds to the brief closing events shown in Fig. 12C. If we assume that the fast component represents the closing events within bursts predicted by scheme R2, then the number of closings per burst is given by the ratio of the amplitudes of the fast and slow components, $0.1/0.9 \approx 0.1$ (see Appendix). Since there must always be one more opening event than the number of closings per burst, we obtain an estimated mean of 1.1 openings per burst or a ratio of 10 for k_{-1}/β . Thus, the absence of dramatic bursting behavior in the lower Ca²⁺ limit can be interpreted as evidence that the rate of Ca²⁺ dissociation, k_{-1} is much faster than the rates for channel opening and closing, β and α . Our estimate of $k_{-1} = 10\beta \approx 5,000 \text{ s}^{-1}$ is probably an underestimate. We cannot distinguish whether the brief closing events at low Ca²⁺ represent intra-burst closures predicted by scheme R2 or whether they belong to the population of "flicker" events that predominate at higher Ca²⁺ (see below).

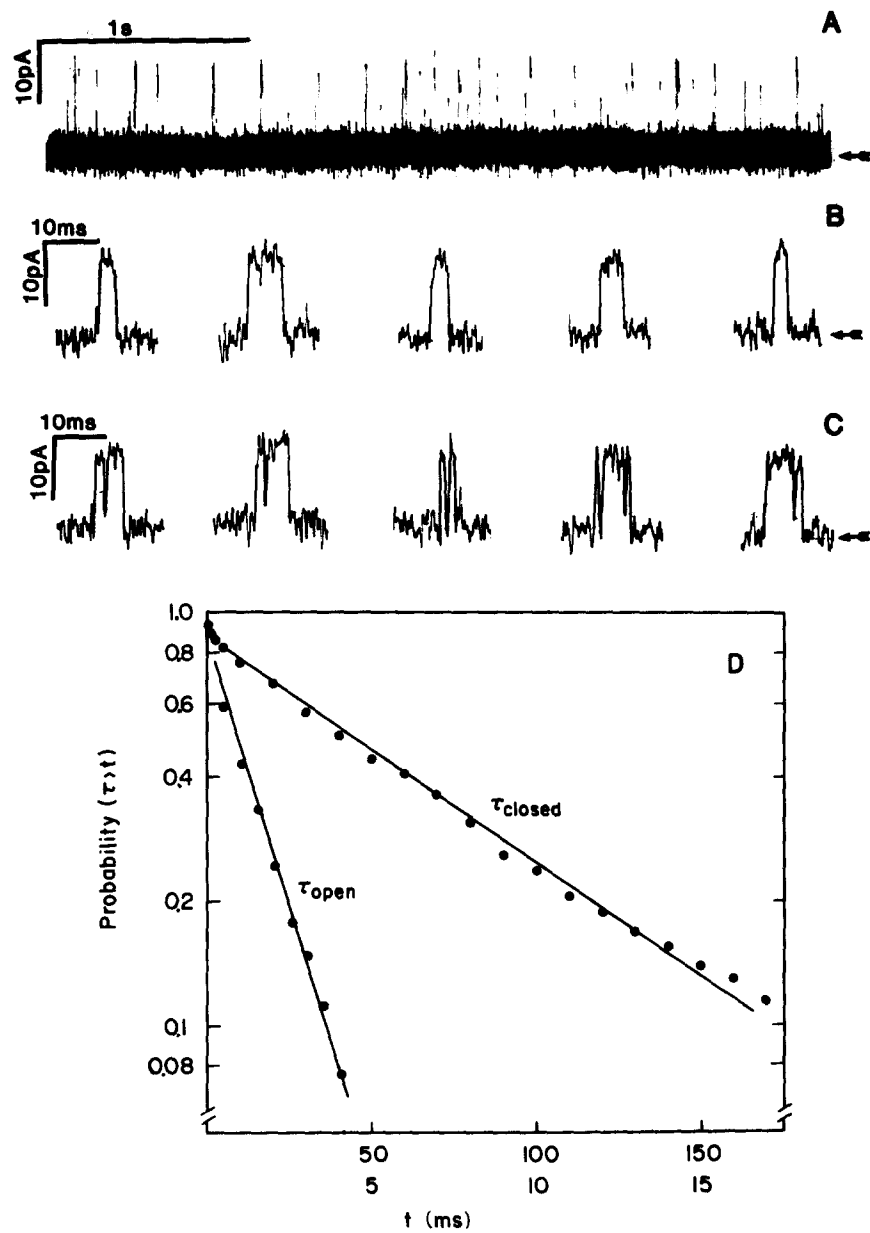
If the rates of Ca²⁺ binding are fast compared with the β/α transition of scheme R1, as the results of Fig. 12 suggest, then the probability distributions predicted by scheme R1 reduce to single-exponential decay laws for both closed- and open-state events. Therefore, our observation of single-exponential probability distributions under most conditions (Fig. 5) is consistent with fast rates of Ca²⁺ binding compared with a slow

FIGURE 11. (*opposite*) Comparison of actual and theoretical open-state probability vs. Ca²⁺ concentration and voltage. The time-averaged (20 s) probability of residence in the open state, P_o , was measured as the simple fraction of time in the open state (●) at various Ca²⁺ concentrations and voltages. P_o (○) was also measured according to Eq. 4 using mean open and closed times obtained by least-square fits of probability distributions as described in Fig. 5. Ca²⁺ concentrations for each curve were as follows from left to right: (A) 1 mM, 39 μ M, 19 μ M, 9 μ M, 5 μ M, 1 μ M; (B) 7.6 mM, 1.6 mM, 560 μ M, 55 μ M, 15 μ M, 1 μ M. Solid lines are theoretical curves calculated from Eq. 3 as derived from scheme R1. Kinetic parameters are best-fit values given in Fig. 9 and Table II. A and B are results of two different channels that correspond to A and B of Fig. 10 and Table II. In C, a Hill plot of data from A (positive voltages, filled symbols) and B (negative voltages, open symbols) is shown. The least-squares slopes of the solid lines in C are as follows from left to right: +50 mV, 1.8; +40 mV, 1.6; +30 mV, 1.7; +20 mV, 1.6; -20 mV, 1.2; -30 mV, 1.1; -40 mV, 1.2; -50 mV, 1.2.

closed-open conformational transition. A more detailed discussion of this point is presented in the Appendix.

Ca²⁺ and Voltage Dependence of the Flicker Process: Possible Interpretations

A different type of bursting behavior exhibited by this channel involves the flicker events discussed in reference to Fig. 4. The unrestricted closed-state probability distribution of Fig. 4B is a clear example of the type of closed-



state distribution expected for a bursting pattern of channel opening. From this figure, the ratio of the amplitudes of the short to long components that represent intra-burst closures and inter-burst closures, respectively, gives a mean value of 1.7 closures or 2.7 openings per burst. Comparison of these results with those of Fig. 12 clearly indicates that bursting behavior is more prevalent at higher open-state probabilities. In the experiment of Fig. 4, for an open-state probability of $P_o = 0.49$, there are 2.7 openings per burst, whereas for Fig. 12 with $P_o = 0.024$, there are only 1.1 openings per burst.

In order to characterize the bursting behavior in more detail, we examined closed-state probability distributions for the same channel at several Ca²⁺ concentrations and holding voltages. At 2.5 kHz resolution we estimate that approximately half of all recognizable flickers are counted by our computer analysis. This counts only those closures reaching 50% of the open-state current level in order to avoid misreading noise as transitions. Therefore, the results based on this method are at least a twofold underestimate of the actual number of flickers per burst. The mean duration of flicker events is <1 ms under all conditions examined and appears to shorten at high Ca²⁺ concentration and large positive potentials. Thus, at P_o values of >0.95 the flicker events visually shorten and disappear from the current records. Despite these limitations, we are able to discern that the number of flickers per burst is approximately a linear function of Ca²⁺ concentration, as shown by the results of Fig. 13. Fig. 13 also shows that at fixed Ca²⁺ concentration, the number of flickers per burst increases as the membrane potential is made more positive.

This type of behavior cannot be explained by scheme R1, which predicts that the number of openings per burst should be independent of Ca²⁺ concentration and should tend to become kinetically indistinguishable at high Ca²⁺, as the Ca²⁺ association binding rates become fast.

To account for such behavior, it is necessary to add at least one additional closed state to scheme R1. One hypothesis for the flicker closures is that they arise from a fast block of the channel caused by Ca²⁺ binding to the open conformations. This hypothesis would predict that the number of flickers per burst should be directly proportional to Ca²⁺ concentration and should

FIGURE 12. (*opposite*) Evidence of bursting behavior in the low Ca²⁺ concentration limit. (A) Section of a current record from a single-channel membrane at 1 μ M *cis* Ca²⁺ concentration and +40 mV. Open-state probability averaged over 31 s was 0.024. 2 kHz filtering. (B) Five examples of the major type of opening events on an expanded time scale. (C) Five examples of rare bursts of opening events. (D) Cumulative probability distribution histograms constructed from the record of A as described in Materials and Methods without exclusion of short-lived closing events. The sampling rate was 2,000 points/s. 421 events were counted for 31 s of total time. Solid lines are drawn by eye and correspond to time constants of 80 ms for the closed state and 2 ms for the open state. The upper and lower time scales correspond to the closed- and open-state distributions, respectively.

also be voltage dependent.³ Another possible hypothesis for the flicker bursts would be to add an additional closed state with two bound Ca^{2+} ions to scheme R1, as part of the gating pathway. In cases where two agonist binding steps precede channel opening, it has been previously shown that bursting behavior proportional to agonist concentration is predicted under certain conditions (Colquhoun and Hawkes, 1981). In this regard, it may be worth exploring the applicability of model 4 of Table I (which includes a doubly bound closed state) as a possible gating scheme that accounts for the flicker behavior. In any case, detailed analysis of the flicker phenomenon will require higher time resolution than that achieved in the present work. For the interpretation of results in this paper, the Ca^{2+} concentration-dependent flicker events can be considered a side reaction occurring from the open-state transitions of scheme R1. This is demonstrated by the results of Fig. 4C, which show that when flickers are eliminated, the probability distribution of the open-state burst length is well described by a single exponential.

Kinetic Heterogeneity

Inspection of the results shown in Fig. 11, A and B, reveals that the two different channels analyzed in these experiments do not exhibit the same Ca^{2+} concentration dependence at a given voltage. For example, at $1 \mu\text{M}$ Ca^{2+} , the channel shown in Fig. 11B is shifted ~ 15 mV more positive along the voltage axis than the channel of Fig. 11A. Also, the best fits obtained for the voltage dependence of the Ca^{2+} dissociation constants for the two channels show some difference (Fig. 10, A and B; Table II). This type of variation appears to be an inherent property of the Ca^{2+} -activated K^+ channels that we have studied in planar bilayers.

Fig. 14 shows the results of a compilation of many experiments in which steady state conductance vs. voltage data were accumulated for different membranes containing one to four channels. Data points for each membrane are plotted individually to show the spread in the voltage dependence for different membranes measured under the same conditions. These results indicate that there is about a 30–50-mV spread for different channels studied under the same conditions. Stated in another way, different channels can vary by as much as 0.8 P_o units at the same voltage and Ca^{2+} concentration. In addition to sample variation between different channels, we have observed that the gating behavior of any given channel is not always constant with time. For example, Fig. 15A shows an instance where a channel gating at a P_o of ~ 0.7 suddenly shifted to a P_o of < 0.1 . On a single-channel level, one might, for example, expect to occasionally observe irreversible inhibition of

³ A similar hypothesis involving fast blockade by suberyldicholine has previously been considered in reference to similar fast flickers observed for acetylcholine receptor channels (Colquhoun and Sakmann, 1981). However, in this case, the hypothesis was eliminated since the number of flickers per burst was not proportional to agonist concentration. In the case of Ca^{2+} -activated K^+ channels, this hypothesis is attractive, especially in light of the successful application of a Ca^{2+} -block model to the long-lived closing phenomenon (Vergara and Latorre, 1983). A fast Ca^{2+} block may also explain the 30% reduction in the apparent single-channel conductance that we observe at high Ca^{2+} concentrations.

channel activity due to a background rate of thermal denaturation or possible proteolytic activity remaining in an impure membrane preparation.⁴ However, these explanations do not totally suffice, since we also observe cases where a given channel suddenly shifts toward a higher probability of being open (e.g., Fig. 15B) or shifts to a different gating rate (e.g., Fig. 15C). Similar phenomena have been reported for the glutamate-activated channel

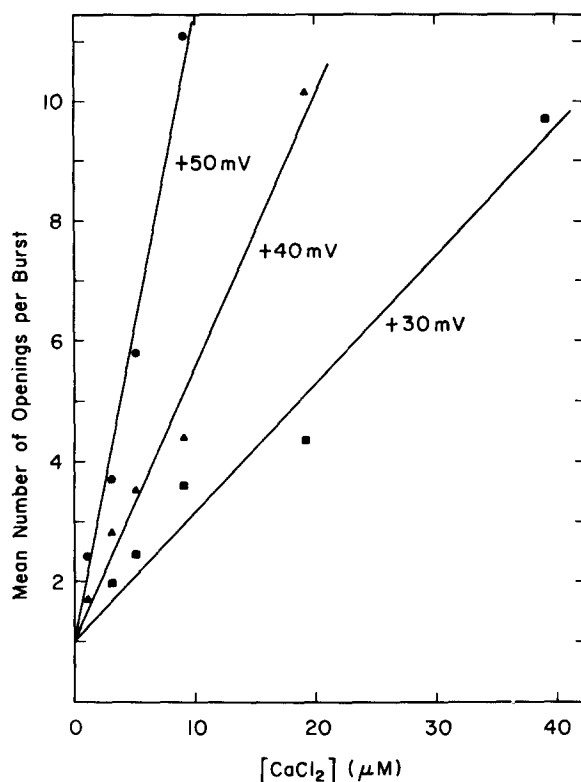


FIGURE 13. Dependence of flicker bursting on Ca²⁺ concentration and voltage. The ordinate axis corresponds to the mean number of openings separated by fast closures <1 ms in duration (averaged over 20 s) at the indicated Ca²⁺ concentration and voltage. The ordinate values are estimates determined as described in the text. Data are shown for a single channel; however, all channels showed similar behavior. The number of transitions used for these calculations ranged from 238 to 666. Solid lines are drawn by eye.

of locust muscle (Gration et al., 1981), where it was proposed that such behavior may arise from inherent time-dependent variations in the gating

⁴ We think that such irreversible inhibition may result from Ag⁺ ions contaminating the bath medium from the silver/silver chloride electrodes, since the use of agar bridges or 1 mM β-mercaptoethanol in the buffer solution seems to reduce spontaneous channel death. Irreversible inhibition by Ag⁺ has previously been noted for the SR K⁺ channel by Miller and Rosenberg (1979).

equilibria (i.e., slow conformational changes). We might also speculate that such behavior could arise from regulatory mechanisms such as dissociable subunits or protein phosphorylation activities that may contaminate these preparations (De Peyer et al., 1982). However difficult such phenomena are

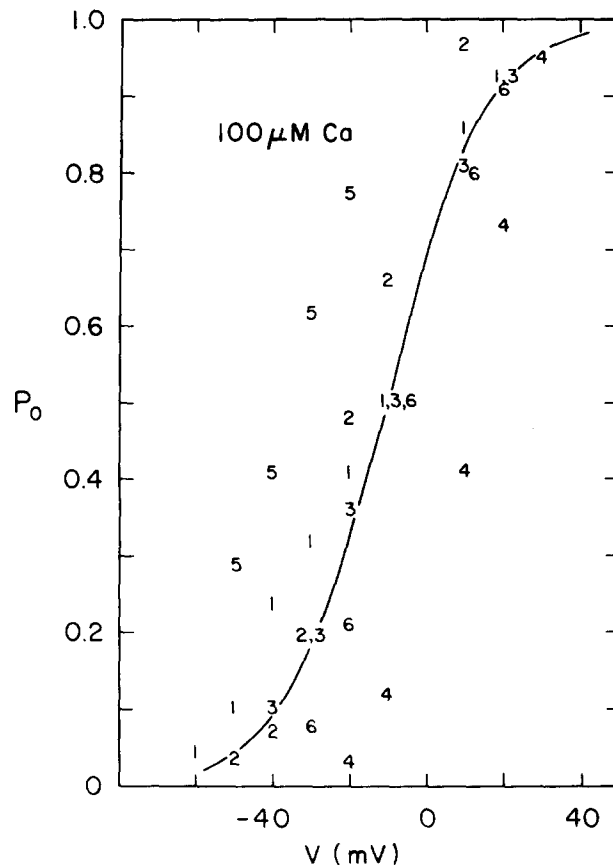


FIGURE 14. Macroscopic Ca^{2+} and voltage dependence of gating behavior. The buffer was 25 mM HEPES-Tris, pH 7.4, 0.1 M KCl. After one to four Ca^{2+} -activated K^+ channels had incorporated, the time-averaged current at various holding voltages was measured using 1 kHz filtering. The ordinate parameter, P_0 , was calculated as the ratio of the measured current to the current expected if all channels in the membrane were fully open. *cis* Ca^{2+} concentration: 100 μ M. Data points are indicated by numerals corresponding to different bilayers. A total of six different bilayers were analyzed. The solid line was calculated by averaging the data.

to study at present, this behavior is not confined to the planar bilayer system. Two laboratories studying the same channel from rat myotubes by patch-clamp techniques have reported similar data scatter and channel heterogeneity (Methfessel and Boheim, 1982; B. Suarez-Isla, personal communication).

DISCUSSION

Identical Behavior of the Ca²⁺-activated Channel in Planar Bilayers and Native Membranes

The present work and results described elsewhere (Latorre et al., 1982; Vergara and Latorre, 1983) provide ample evidence that the channel we are studying in planar bilayers is identical to the Ca²⁺-activated K⁺ channel from muscle plasma membrane characterized by patch-clamp recording (Barret et al., 1982; Methfessel and Boheim, 1982). Upon transfer to a Mueller-Rudin

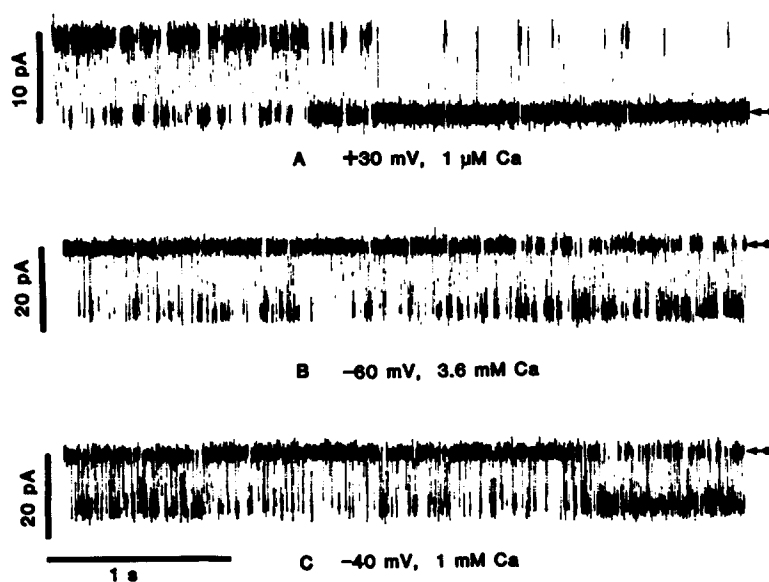


FIGURE 15. Examples of unstable gating behavior. Current records of different Ca²⁺-activated K⁺ channels in pure PE bilayers are shown at the indicated Ca²⁺ concentration and holding voltage. 1 kHz filtering. Time proceeds from left to right in all traces. (A) Example of an abrupt shift to a lower open-state probability. (B) Example of a shift to a higher open-state probability. Compare the left vs. right side of the trace. (C) Example of a shift to an erratic, but lower, open-state probability in the middle of the trace and a shift back to a higher probability at the right side of the trace. Arrows indicate zero-current level.

bilayer, this channel retains the same cation selectivity and single-channel conductance and also exhibits the same variety of kinetic phenomena as the channel observed in myotubes. The results obtained for the rat myotube channel indicate that it is open 50% of the time at a voltage of +15 mV for a Ca²⁺ concentration of 2–5 μM. We find that a sampling of channels in PE bilayers has a 50% open-state probability at voltages ranging from +15 to +55 mV at 3 μM Ca²⁺ (Fig. 14). However, we found that in pure PS bilayers, the *P*_o vs. voltage curves are shifted to more negative potentials and coincide with the reported data from membrane patches (E. Moczydlowski, C. Ver-

gara, and R. Latorre, manuscript in preparation). Therefore, differences in lipid composition can explain the difference in $[Ca^{2+}]$ sensitivities we have observed between the native and reconstituted channel. The gating kinetics of the rat and rabbit channel in bilayers have not been compared quantitatively. However, at a gross level, the behavior of the channels from the two species is indistinguishable. We note here that a similar channel from anterior pituitary cells was reported to have a 50% open-state probability shifted by ~ 50 mV to more negative voltages than the rat myotube channel (Wong et al., 1982). Thus, it is possible that other species-specific or tissue-specific differences, in addition to lipid composition, may affect the relative Ca^{2+} affinities of these channels.

At first glance, it appears surprising that the function of a biological channel (i.e., an integral membrane protein) is not significantly perturbed upon transfer to a Mueller-Rudin phospholipid bilayer. This is surprising inasmuch as this type of bilayer contains a large mole fraction of decane and is ~ 18 Å thicker than a bilayer without decane (Haydon et al., 1977).⁵ Actually, we are not aware of any evidence indicating that these levels of decane significantly perturb channels. On the contrary, although *n*-alkanes shorter than C_8 reversibly depress the action potential of squid axons, longer-chain alkanes have little effect (Haydon et al., 1977). Also, in a case where virtually solvent-free decane-containing membranes have been directly compared for the SR K^+ channel, there is little difference in channel behavior (Labarca et al., 1980). Thus, it seems to us reasonable to assume that the planar bilayer formed from a phospholipid solution in decane is a good analogue of the cell membrane from which these channels are derived.

Kinetic Model for the Primary Gating Mode

Scheme R1 is proposed as a minimum model for the Ca^{2+} - and voltage-dependent activation kinetics of the channel under study. This model is based on the following evidence.

(a) The mean closed time (excluding brief flickers) is a linear function of $1/[Ca^{2+}]$. The mean open time (length of bursts interrupted by brief flickers) is a linear function of $[Ca^{2+}]$.

(b) In the limit of zero $[Ca^{2+}]$, the mean open times at all voltages converge to the same value, $1/\alpha$. In the limit of infinite Ca^{2+} , the mean closed times at all voltages converge to the same value, $1/\beta$. The slopes of linear functions of $\bar{\tau}_o$ vs. $[Ca^{2+}]$ and $\bar{\tau}_c$ vs. $1/[Ca^{2+}]$ are exponential functions of voltage.

(c) The dependence of the equilibrium probability of the open state on Ca^{2+} concentration and voltage is quantitatively predicted by scheme R1.

(d) The observation of single-exponential open- and closed-state probability distributions is predicted by scheme R1 if the K_1 and K_2 Ca^{2+} binding reactions are fast compared with the β/α conformational transition. The appearance

⁵ It might be argued that decane is excluded from contact with channels by tightly bound lipid carried over from the native membrane during vesicle fusion. However, since we do find a difference in Ca^{2+} sensitivity in PS vs. PE bilayers (E. Moczydłowski, C. Vergara, and R. Latorre, manuscript in preparation), it appears that the channel does sense the lipid environment of the planar bilayer.

of a second fast component in these distributions at intermediate Ca²⁺ concentrations is also consistent with scheme R1, since the resolution of two closed and two open states is favored in this limit.

The kinetic results in planar bilayers are in agreement with the available data from native membrane patches. For the myotube channel at +60 mV, log-log plots of $\bar{\tau}_o$ vs. [Ca²⁺] have a slope of +1 and log-log plots of $\bar{\tau}_c$ vs. [Ca²⁺] have a slope of -1 (Methfessel and Boheim, 1982). These results agree with ours (point *a* above).

We have analyzed the Ca²⁺ dependence of the open-closed equilibrium constant of this channel in an empirical fashion as log-log plots of K_{eq} vs. Ca²⁺ concentration. We find that slopes of such plots have values >1.0, ranging from 1.2 to 2.0 for the rat and rabbit channel in bilayers. In close agreement, the theoretical values for these slopes based on the model derived from the dwell time analysis were 1.4 at -50 mV and 1.7 at +50 mV. In a comparison of their data with data from other laboratories, Methfessel and Boheim (1982) found that the slopes of such plots ranged from 1.6 to 2.5 for the Ca²⁺-activated channel from muscle. This suggests that the number of Ca²⁺ ions necessary to activate a channel fully cannot be very different in lipid bilayers than in cell membrane patches.

In other studies of this channel, emphasis is placed on slope values of >2.0 to propose the involvement of three Ca²⁺ ions in the gating process (Barret et al., 1982; Wong et al., 1982). These data are also described as consistent with a third-power Ca²⁺ relationship that has been observed in macroscopic experiments on invertebrate neurons (Meech and Thomas, 1980). In our case, the pure first-order and reciprocal first-order Ca²⁺ concentration dependence of the mean open and closed times, respectively, strongly suggests the participation of only two Ca²⁺ ions in the gating process. Although we sometimes observe slope values slightly >2.0, this appears to be due to scatter in the data caused by slight gating shifts during the experiment. We conclude that our derived relationships are adequate to account for the observed Ca²⁺ dependence of the channel from muscle plasma membranes.

The voltage dependence of the channel equilibrium has been previously modeled as a two-state open-closed equilibrium. In this case, the natural logarithm of K_{eq} is a linear function of voltage (Lecar et al., 1975). Slopes of these plots for the data of different laboratories working with muscle membrane range from 2.0 to 2.3, as summarized by Methfessel and Boheim (1982). Wong et al. (1982), working with anterior pituitary cells, report a value of 2.8 for this slope. Our model also gives a nearly linear relationship for plots of $\ln K_{eq}$ vs. V and the slopes of these plots range from 3.0 at 1 μ M Ca²⁺ to 2.4 at 1 mM Ca²⁺. Therefore, the values based on our model and the reported slope values from membrane patches agree within experimental error. Better agreement would result if the δ values of Table II were slightly overestimated.

Other Models Are Also Possible But They Are Less Economical

Methfessel and Boheim (1982) have proposed a kinetic scheme described as an "activation-blockade" model of channel gating. This model is formally

equivalent to our scheme R1 in that it predicts the same dependence of the mean open and mean closed times on Ca^{2+} concentration. However, their model assumes that the Ca^{2+} binding constants are voltage independent and that the closed-open conformational transition is voltage dependent. We find the opposite behavior. They also propose that Ca^{2+} activates the channel by binding to a negatively charged voltage-dependent gate that normally blocks the channel. Although these authors have used a similar approach to the kinetic analysis of this channel, we have arrived at a different interpretation of the results (see below).

Although scheme R1 has the least number of intermediate states and reactions required to account for the results, more complicated models that predict the same behavior can be proposed. For example, model 4 of Table I could be fit to our data if $\alpha_3 \ll \alpha_2$, $\beta_3 \ll \beta_2$, and $K_2 \gg K_1$. Also scheme R1 does not uniquely specify the functional unit of the channel gating structure since a dimer with cooperative binding between two identical Ca^{2+} sites on each monomer could give the same kinetic behavior as a monomeric functional unit with two distinct Ca^{2+} binding sites. In addition, by introducing an extra voltage-dependent closed-closed transition to scheme R1 preceding Ca^{2+} binding to the closed state, the K_1 binding transition can be made voltage independent to give the same predicted behavior as the observed voltage dependence of the mean closed time. Thus, we cannot uniquely conclude that the actual Ca^{2+} binding rates are voltage dependent from the present results. On the other hand, we have no direct evidence for these additional states.

Toward a Molecular Understanding of the Gating Process

The data of Fig. 9, *A* and *B*, are evidence that the actual opening and closing conformational transitions of the channel are voltage independent. This result is surprising considering previous notions of voltage-dependent gating. Voltage-dependent ionic currents of biological membranes are usually explained in terms of voltage-sensing charges or dipoles coupled to a gating structure that blocks access to a pore through the membrane. When an electric field of the right polarity is applied across the membrane, the dipole tends to align itself with the field and thus opens the gate. Since the Ca^{2+} -activated K^+ channel has an appreciable voltage dependence (an e-fold change in its open-closed equilibrium per 12 mV), we expected it to exhibit a typical voltage-dependent open-closed conformational transition. On the other hand, agonist-dependent ion channels such as the acetylcholine receptor and the glutamate receptor of invertebrates are essentially voltage independent, and the opening of these channels is thought to involve a simple, weakly voltage-dependent conformational change induced by agonist binding (for a review see Adams, 1981). Thus, the Ca^{2+} -activated K^+ channel can be related to neurotransmitter receptor channels inasmuch as Ca^{2+} plays the agonist role. However, as opposed to the latter type of channels, the agonist binding reactions in the Ca^{2+} -activated channels are voltage dependent.

Although scheme R1 proposes that the K_1 and K_4 binding reactions are

voltage dependent, we have not determined whether the actual Ca²⁺ association and dissociation rates are voltage dependent. However, there is a precedent for voltage-dependent binding rates of charged molecules in various studies of channel-blocking agents (e.g., Woodhull, 1973; Neher and Steinbach, 1978; Coronado and Miller, 1979; Miller, 1982; Vergara and Latorre, 1983). These examples serve to focus on a possible molecule interpretation for voltage-dependent Ca²⁺ binding to the Ca²⁺-activated K⁺ channel.

Three Hypotheses to Explain Voltage-dependent Ca²⁺ Binding Constants

If we assume that the rates of Ca²⁺ binding to the activation sites are voltage dependent, then a conventional interpretation implies that these sites are located in an electric field. The derived values of $\delta_1 \approx 0.75$ and $\delta_4 \approx 0.95$ may also imply that these sites are located deep in the field, i.e., they “sense” most of the field. We can think of two possible locations for sites of this type. In the first case, they may be located in the mouth of the channel itself, perhaps near the conduction sites for K⁺ entering the channel from the *cis* side. This possibility is somewhat unattractive because of the repulsive forces exerted by two divalent and one monovalent cation crowded together in a small area. It would require at least five negative charges distributed throughout these sites to neutralize the charges of incoming ions and prevent their mutual repulsion. However, this picture should not totally be ruled out in light of the evidence for “wide mouths” of these channels (Latorre and Miller, 1983). A wide mouth leading to the conduction pathway might allow enough room for these sites to reside in the same cleft of the protein in electrostatic harmony.

A second possibility would be to propose an activation cleft for the location of the Ca²⁺ activation sites that would be distinct from the actual channel mouth or conduction pathway. There is some evidence for this possibility. By comparing the Ca²⁺ concentration dependence of the activation kinetics and the conductance vs. K⁺ concentration dependence in phosphatidylethanolamine vs. phosphatidylserine bilayers, we find that the Ca²⁺ activation sites are more sensitive to the membrane surface potential than the K⁺ conduction sites (E. Moczydlowski, C. Vergara, and R. Latorre, manuscript in preparation). This result indicates that the Ca²⁺ activation sites are closer to the lipid head groups than the K⁺ conduction site and thus implies separate binding clefts. For these two models, we would expect that either or both of the Ca²⁺ binding association and dissociation rates are voltage dependent. In both of these models, Ca²⁺ binding would activate gating by inducing conformational changes that stabilize the open states of the channel, i.e., by lowering the activation energy of opening.

A third possibility is that the actual Ca²⁺ binding rates are voltage independent. In this case, a dipole in the membrane distant from but coupled to the Ca²⁺ binding sites would cause the Ca²⁺ binding affinity to be modulated by an applied electric field. This explanation would invoke changes in protein structure to explain the coupling between voltage and apparent Ca²⁺ binding

affinity, rather than a direct influence of the electric field on the movement of Ca^{2+} ions. This possibility seems the least attractive hypothesis, because there is no precedent for such a mechanism, as far as we are aware.

APPENDIX

Predicted Behavior in the Fast Binding Limit

The unconditional closed-time probability distribution of a kinetic model such as schemes R1 or R2 is explicitly given as a sum of two exponentials (Colquhoun and Hawkes, 1981). The cumulative probability form, P , is as follows:

$$P = A_1 \exp(-\lambda_1 t) + A_2 \exp(-\lambda_2 t); \quad (5)$$

$$\lambda_1(-), \lambda_2(+) = 0.5[b \pm (b^2 - 4c)^{1/2}];$$

$$b = \beta + k_1[\text{Ca}] + k_{-1} = \lambda_1 + \lambda_2;$$

$$c = \beta k_1[\text{Ca}] = \lambda_1 \lambda_2;$$

$$A_1 = (\lambda_2 - \beta)/(\lambda_2 - \lambda_1), A_2 = (\beta - \lambda_1)/(\lambda_2 - \lambda_1).$$

The unconditional mean of this sum of two exponential distribution is equal to $\beta^{-1}(1 + K_1/[\text{Ca}])$, regardless of the values for β , k_{-1} , and $[\text{Ca}]k_1$. However, it can also be shown analytically that when the Ca^{2+} binding rates are fast compared with the rate of channel opening, $k_1[\text{Ca}] + k_{-1} \gg \beta$, then the probability distribution is dominated by the first term of Eq. 5 and approaches a single exponential with the same mean as the sum of two-exponential distribution. Specifically, in this fast binding limit: A_1 approaches 1.0, λ_1^{-1} approaches $\beta^{-1}(1 + K_1/[\text{Ca}])$, $A_2 \rightarrow 0$ and λ_2^{-1} becomes very short. Therefore, the intermediate steps of Ca^{2+} binding are kinetically indistinguishable in the fast binding regime and the two closed states with zero and one bound Ca^{2+} may be grouped as a single state in rapid equilibrium. An equivalent analysis can be made for the open-state distribution of scheme R1 since this model has two open states with only one pathway of closing.

Thus, if scheme R1 is a valid model for the gating activation pathway, we must also conclude that the rates of Ca^{2+} binding are fast compared with the conformational transitions. At high Ca^{2+} and P_o values where the $K_1[\text{Ca}]$ and $k_4[\text{Ca}]$ rates are large, we expect to observe single-exponential distributions for the open and closed states. Conversely, at low Ca^{2+} and P_o values, a distribution following a sum of two exponentials can be expected, depending on the magnitude of k_{-1} and k_{-4} . We observe excellent fits to single exponentials (excluding short-lived flicker closings) at high Ca^{2+} and detect a small but significant second component for both closed- and open-state distributions at low Ca^{2+} (see also data of Barret et al., 1982). These observations reinforce the validity of scheme R1 (i.e., it is evidence for at least two closed and two open states).

According to this interpretation, the short component of the open-state population at low Ca^{2+} mainly reflects short residence times in the singly bound open state, where the long component reflects mixed residence in the singly and doubly bound open states. Unfortunately, fast binding makes it difficult to estimate the actual values for the Ca^{2+} binding rate constants from the present experiments. This would clearly be of interest in determining the relative voltage dependence of the Ca^{2+} association and dissociation reactions.

We thank Drs. R. Coronado and C. Vergara for many stimulating discussions on channels. We also thank Drs. C. Miller and D. Benos for critical reading of this manuscript. Dr. Miller

cheerfully tolerated our use of his computer. Invaluable secretarial help was provided by Marianita Sanchez.

This work was supported by NIH grants GM-28992 and GM-25277. E. Moczydlowski was supported by a postdoctoral fellowship from the Muscular Dystrophy Association and National Institutes of Health fellowship 5 F32 NS-06697.

Received for publication 2 February 1983 and in revised form 18 April 1983.

REFERENCES

- Adams, P. R. 1981. Acetylcholine receptor kinetics. *J. Membr. Biol.* 58:161–174.
- Adams, P. R., A. Constanti, D. A. Brown, and R. B. Clark. 1982. Intracellular Ca²⁺ activates a fast voltage-sensitive K⁺ current in vertebrate sympathetic neurons. *Nature (Lond.)*. 296:746–749.
- Barret, J. N., K. L. Magleby, and B. S. Pallota. 1982. Properties of single calcium-activated potassium channels in cultured rat muscle. *J. Physiol. (Lond.)*. 331:211–230.
- Colquhoun, D., and A. G. Hawkes. 1977. Relaxation and fluctuation of membrane currents that flow through drug operated channels. *Proc. R. Soc. Lond. B Biol. Sci.* 199:231–262.
- Colquhoun, D., and A. G. Hawkes. 1981. On the stochastic properties of single ion channels. *Proc. R. Soc. Lond. B Biol. Sci.* 211:205–235.
- Colquhoun, D., and B. Sakmann. 1981. Fluctuation in the microsecond time range of current through single acetylcholine receptor ion channels. *Nature (Lond.)*. 294:464–466.
- Conti, F., and E. Neher. 1980. Single channel recordings of K⁺ currents in squid axons. *Nature (Lond.)*. 285:140–143.
- Coronado, R., and C. Miller. 1979. Voltage-dependent cesium blocking of a potassium channel derived from fragmented sarcoplasmic reticulum. *Nature (Lond.)*. 280:807–810.
- De Peyer, J. E., A. B. Cachelin, I. B. Levitan, and H. Reuter. 1982. Ca²⁺-activated K⁺ conductance in internally perfused snail neurones is enhanced by protein phosphorylation. *Proc. Natl. Acad. Sci. USA*. 79:4207–4211.
- Gration, K. A. F., J. J. Lambert, R. Ramsey, and P. N. R. Usherwood. 1981. Non-random openings and concentration-dependent lifetimes of glutamate-gated channels in muscle membranes. *Nature (Lond.)*. 291:423–425.
- Haydon, D. A., B. M. Hendry, S. R. Levinson, and J. Requena. 1977. Anesthesia by the *n*-alkanes. A comparative study of nerve impulse blockage and the properties of black lipid bilayer membranes. *Biochim. Biophys. Acta*. 470:17–34.
- Labarca, P., R. Coronado, and C. Miller. 1980. Thermodynamic and kinetic studies of the gating behavior of a K⁺-selective channel from the sarcoplasmic reticulum membrane. *J. Gen. Physiol.* 76:397–424.
- Latorre, R., and C. Miller. 1983. Conduction and selectivity in K⁺ channels. *J. Membr. Biol.* In press.
- Latorre, R., C. Vergara, and C. Hidalgo. 1982. Reconstitution in planar lipid bilayers of a Ca²⁺-dependent K⁺ channel from transverse tubule membranes isolated from rabbit skeletal muscle. *Proc. Natl. Acad. Sci. USA*. 79:805–809.
- Lecar, H., G. Ehrenstein, and R. Latorre. 1975. Mechanisms for channel gating in excitable bilayers. *Ann. NY Acad. Sci.* 264:304–313.
- Marty, A. 1981. Ca²⁺-dependent K⁺ channels with large unitary conductance in chromaffin cell membranes. *Nature (Lond.)*. 291:497–500.
- McLaughlin, S. 1977. Electrostatic potentials at membrane-solution interfaces. *Curr. Top. Membr. Transp.* 9:71–144.

- Meech, R. W., and R. C. Thomas. 1980. Effect of measured calcium chloride injections on the membrane potential and internal pH of snail neurones. *J. Physiol. (Lond.)*. 298:111-129.
- Methfessel, C., and C. Boheim. 1982. The gating of single calcium-dependent potassium channels is described by an activation-blockage mechanism. *Biophys. Struct. Mech.* 9:35-60.
- Miller, C. 1982. Bis-quaternary ammonium blockers as structural probes of the sarcoplasmic reticulum K⁺ channel. *J. Gen. Physiol.* 79:869-891.
- Miller, C., and R. L. Rosenberg. 1979. A voltage-gated cation conductance channel from fragmented sarcoplasmic reticulum. Effect of transition metal ions. *Biochemistry*. 18:1138-1145.
- Moczydlowski, E., and R. Latorre. 1983. Saxitoxin and ouabain binding activity of isolated skeletal muscle membrane as indicators of surface origin and purity. *Biochim. Biophys. Acta*. In press.
- Mueller, P., and D. O. Rudin. 1969. Translocators in bimolecular lipid membranes: their role in dissipative and conservative bioenergy transductions. *Curr. Top. Membr. Transp.* 3:157-249.
- Neher, E., and J. H. Steinbach. 1978. Local anesthetics transiently block currents through single acetylcholine-receptor channels. *J. Physiol. (Lond.)*. 277:153-176.
- Pallotta, B. S., K. L. Magleby, and J. N. Barret. 1981. Single channel recordings of a Ca²⁺-activated K⁺ current in rat muscle cell culture. *Nature (Lond.)*. 293:471-474.
- Roseblatt, M., C. Hidalgo, C. Vergara, and N. Ikemoto. 1981. Immunological and biochemical properties of transverse tubule membranes isolated from rabbit skeletal muscle. *J. Biol. Chem.* 256:8140-8148.
- Sakmann, B., J. Patlak, and E. Neher. 1980. Single acetylcholine-activated channels show burst-kinetics in presence of desensitizing concentrations of agonist. *Nature (Lond.)*. 286:71-73.
- Sigworth, F. J., and E. Neher. 1980. Single Na⁺ channel currents observed in cultured rat muscle cells. *Nature (Lond.)*. 297:447-449.
- Vergara, C., and R. Latorre. 1983. Kinetics of Ca²⁺-activated K⁺ channels from rabbit muscle incorporated into planar bilayers: evidence for a Ca²⁺ and Ba²⁺ blockade. *J. Gen. Physiol.* 82:543-568.
- Wong, B. S., H. Lecar, and M. Adler. 1982. Single calcium-dependent potassium channels in clonal anterior pituitary cells. *Biophys. J.* 39:313-317.
- Woodhull, A. M. 1973. Ionic blockage of sodium channels in nerve. *J. Gen. Physiol.* 61:687-708.